5/13/98
ORIGINAL

MICROMACHINED STIMULATING ELECTRODES

Quarterly Report #10

(Contract NIH-NINDS-N01-NS-5-2335)

January - March 1998

Submitted to the

Neural Prosthesis Program
National Institute of Neurological Disorders and Stroke
National Institutes of Health

by the

Center for Integrated Sensors and Circuits
Department of Electrical Engineering and Computer Science
University of Michigan
Ann Arbor, Michigan
48109-2122

April 1998

MICROMACHINED STIMULATING ELECTRODES

Summary

This program seeks to develop a family of two- and three-dimensional active stimulating probes for use in neural prostheses. Two active probes, STIM-1B (monopolar) and STIM-1A (bipolar) have been completed. A four-channel 64-site multipolar probe, STIM-2B is now being completed. This probe allows each of four externally-generated currents to be steered to one of 16 sites under the direction of a digital address delivered to the probe. A three-dimensional version of this probe, STIM-3B, is also nearing completion. Following these probes, the design of a 64-site 8-channel probe, STIM-2, will be iterated, and this probe will also be fabricated, completing this second-generation family of devices.

During the past quarter, we continued to explore the removal of parylene from iridium sites using laser ablation. Site areas ranging from $100\mu m^2$ to $400\mu m^2$ were created on a larger metal site using ablation. The surface was cleaned after ablation using an oxygen plasma, and the resulting sites were used for single-unit recording in cerebellum. The sites performed well, indicating that the ablation procedure is able to fully open sites in probes that have been coated with parylene. This allows the use of parylene as an outer conformal coating on penetrating probes as well as its use on ribbon-based electrode arrays suitable for cochlear prostheses. We have also completed process development on the possible use of a porous silicon layer for probe fabrication. This layer would be used under the basic probe structure and would permit release of the probe using a room-temperature front-side etch. The final process developed uses a p+ diffusion to produce the porous sacrificial layer. It allows circuitry to be distributed on the probe shanks as well as on the rear of the probe.

We have successfully fabricated a run of STIM-1A, -1B, -2, -2B, and -3B probes. As of this writing, one wafer of the -2B/3B probes has been taken to the completion of circuit processing and is found to be completely functional, including the per-channel recording amplifiers. We plan to release these probes from the wafer during the next two weeks and then to complete processing on the other probe wafers. We then anticipate using the probes for a number of in-vivo tests before going back to iterate the design of STIM-2 to complete this second-generation family of probes.

MICROMACHINED STIMULATING ELECTRODES

1. Introduction

The goal of this research is the development of active multichannel arrays of stimulating electrodes suitable for studies of neural information processing at the cellular level and for a variety of closed-loop neural prostheses. The probes should be able to enter neural tissue with minimal disturbance to the neural networks there and deliver highly-controlled (spatially and temporally) charge waveforms to the tissue on a chronic basis. The probes consist of several thin-film conductors supported on a micromachined silicon substrate and insulated from it and from the surrounding electrolyte by silicon dioxide and silicon nitride dielectric films. The stimulating sites are activated iridium, defined photolithographically using a lift-off process. Passive probes having a variety of site sizes and shank configurations have been fabricated successfully and distributed to a number of research organizations nationally for evaluation in many different research preparations. For chronic use, the biggest problem associated with these passive probes concerns their leads, which must interface the probe to the outside world. Even using silicon-substrate ribbon cables, the number of allowable interconnects is necessarily limited, and yet a great many stimulating sites are ultimately desirable in order to achieve high spatial localization of the stimulus currents.

The integration of signal processing electronics on the rear of the probe substrate (creating an "active" probe) allows the use of serial digital input data which can be demultiplexed on the probe to provide access to a large number of stimulating sites. Our goal in this area is to develop a family of active probes capable of chronic implantation in tissue. For such probes, the digital input data must be translated on the probe into per-channel current amplitudes which are then applied to the tissue through the sites. Such probes generally require five external leads, virtually independent of the number of sites used. As discussed in previous reports, we have designed a series of active probes containing CMOS signal processing electronics. Two of these probes have been completed and are designated as STIM-1A and STIM-1B. A third probe, STIM-2, is now undergoing a final iteration and is a second-generation version of our original high-end first-generation design, STIM-1. All three probes provide 8-bit resolution in digitally setting the per-channel current amplitudes. STIM-1A and -1B offer a biphasic range using ±5V supplies from 0μA to ±254μA with a resolution of 2μA, while STIM-2 has a range from 0 to ±127μA with a resolution of 1μA. STIM-2 offers the ability to select 8 of 64 electrode sites and to drive these sites independently and in parallel, while STIM-1A allows only 2 of 16 sites to be active at a time (bipolar operation). STIM-1B is a monopolar probe, which allows the user to guide an externally-provided current to any one of 16 sites as selected by the digital input address. The high-end STIM-2 contains provisions for numerous safety checks and for features such as remote impedance testing in addition to its normal operating modes. It also offers the option of being able to record from any one of the selected sites in addition to stimulation. It will be the backbone of a multi-probe three-dimensional (3D) 1024-site array (STIM-3) now in development. A new probe, STIM-2B, is currently being added to this set. It offers 64-site capability with off-chip generation of the stimulus currents for four separate channels. These channels are organized in four groups so that each current can be directed to any of the 16 sites in its group, and the site can be programmed for either stimulation or recording. This probe will be available in both 2D and 3D versions (as STIM-2B/3B).

During the past quarter, we have continued to fabricate passive probe structures for internal and external users. We have also continued to explore site definition on probes coated with parylene using laser ablation. The development of a process for probe formation using porous silicon as an alternative to the boron diffusion now used has been completed. Finally, the STIM-2b/-3B probes have been refabricated successfully and have been carefully characterized electrically. The results in each of these areas are described more fully in the sections below.

2. *Use of Parylene Ablation for Post-Processing Site Formation*

In the previous quarterly report, we reported on our collaboration with PI-Medical in coating our stimulating electrodes with parylene and then ablating smaller openings in a large site (SX-04, 4000μm^2) to define custom-sized sites (10x10, 15x15, and 20μm x 20μm). We had not attempted to record from these electrodes as of the past quarterly report. Since then, we have been successful in obtaining recordings with them (Fig. 1). These data were recorded in the cerebellum. Channel 1 is at the top, with channel 5 at the bottom of the graph. Channels 1 and 5 have 10μm x 10μm site openings, channels 2 and 4 have 15μm x 15μm ablations, and channel 3 has a 20μm x 20μm site. The RMS noise for a given ablated opening size is shown in Fig. 2. On average, the 10μm sites (channels 1 and 5) have the highest noise level, the 15μm sites (channels 2 and 4) have the next largest and the 20μm sites (channel 3) have the smallest noise level, as should be expected. These data are also consistent with impedance data reported earlier ($9.98x10^4$ for 20μm site, $1.52x10^5$ for 15μm site and $3.12x10^5$ for 10μm site). The data is consistent in showing that parylene can be ablated from sites and, when cleaned with an oxygen plasma, the resulting site surface produces high-quality recordings. This opens up the possibility of using an outer coating of parylene on the probes as an outer encapsulant or, in the case of ribbon cables, as a strengthening agent. This may be very useful in a number of downstream probe applications.

3. *Porous Silicon Micromachining Process Development*

Efforts on the characterization and development of a micromachining process using a porous silicon sacrificial layer have continued. As previously reported, this process is one of several options being investigated as a means for increasing active probe yield and foundry compatibility. This particular option provides an etch-stop on all sides of circuit areas, including underneath, where there is currently no stop provided in the active probe process. Additionally, since only a lightly-doped etch-stop is required, this process provides the option of moving some circuitry from the back ends of probes to their shanks, helping to reduce back-end profiles. The resulting probes can be released from the wafer from the front side of the wafer and can be released using a room temperature etch.

During this past quarter, a double-layer selective epitaxial silicon (epi) growth process was developed in conjunction with DIMES (the Delft Institute of MicroElectronics and Submicron Technology) at Delft University, The Netherlands. It allows the fabrication of double-supply CMOS circuitry on the micromachined probes, while maintaining a grounded outer layer. It also provides the option for using either a p-well process, or a more foundry-compatible n-well process, depending on the doping profile chosen. Trenches are first dry-etched into a wafer to define the shapes of the probes, and the epi is doped as it is grown to refill these trenches.

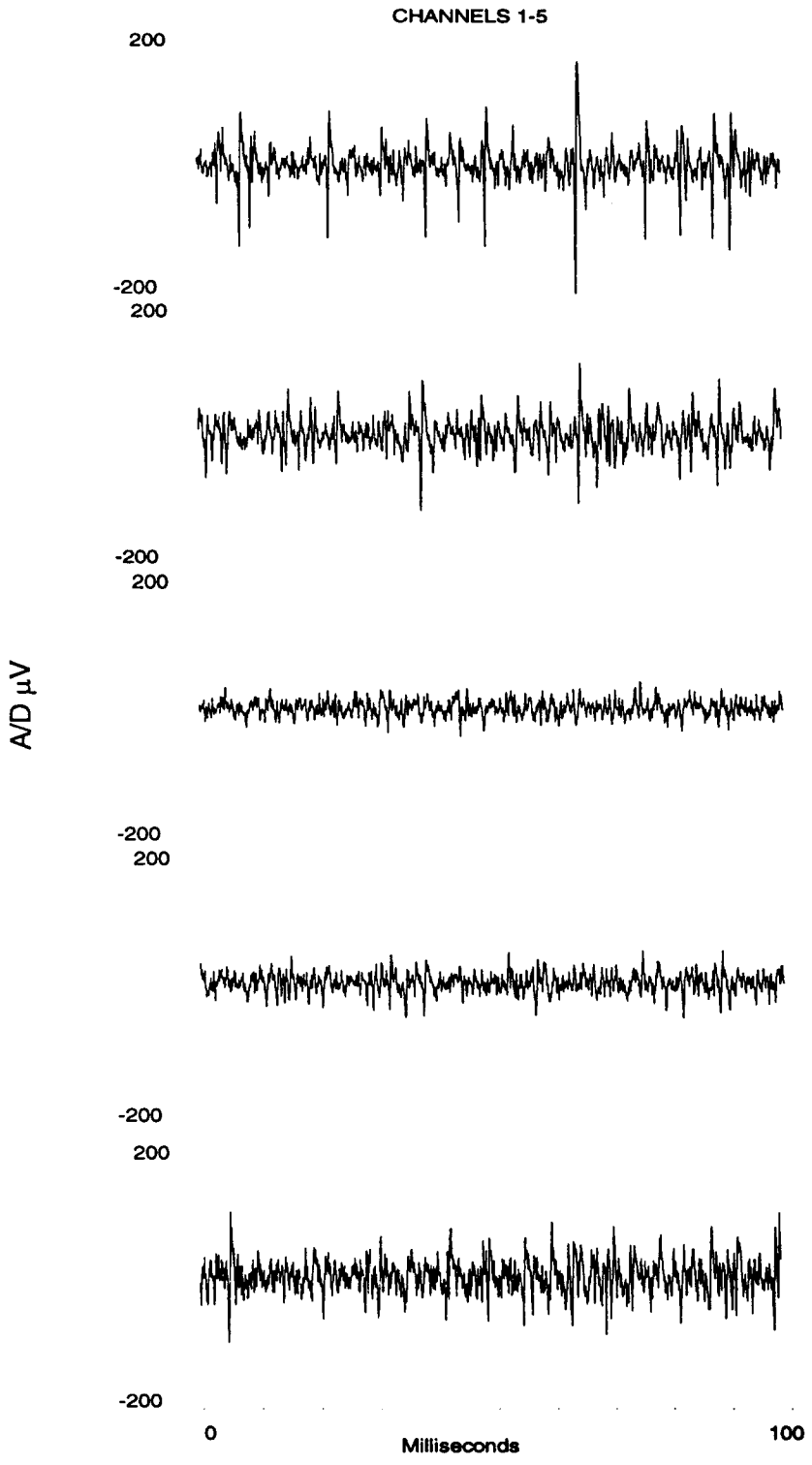

Fig. 1: Recordings obtained from guinea pig cerebellum using site sizes defined by laser ablation of parylene.

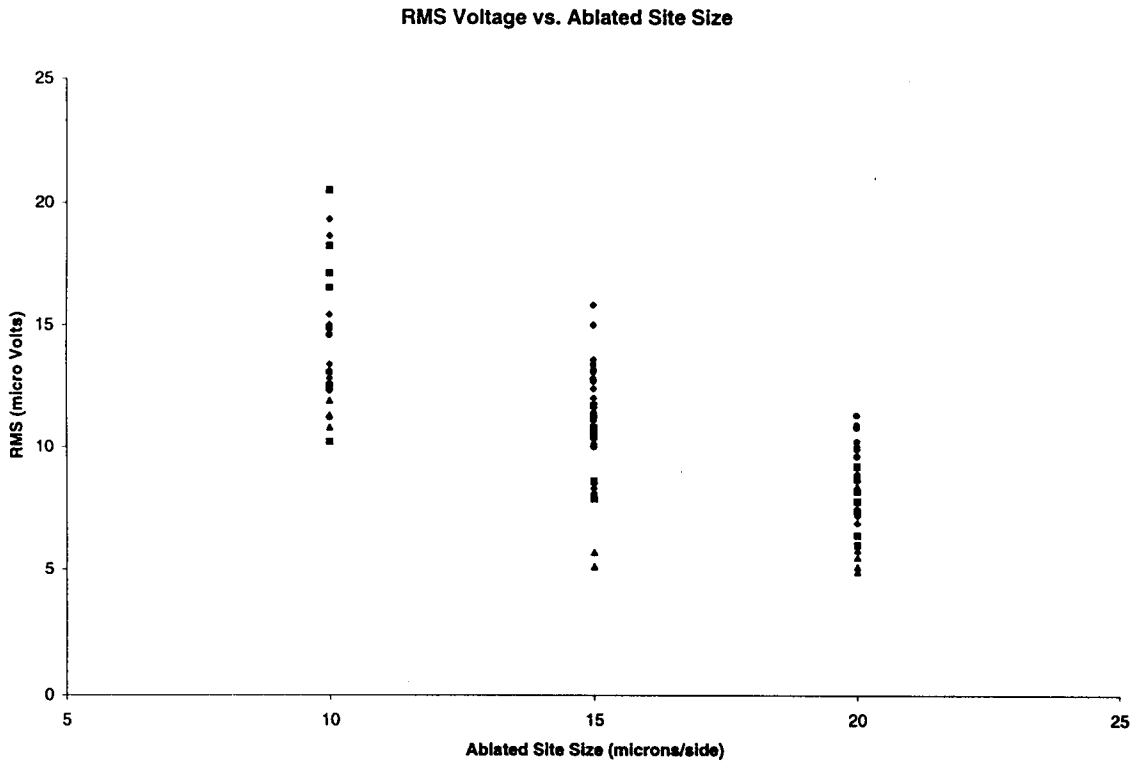

Fig. 2: Rms noise voltage from parylene ablated sites on a multisite recording probe as a function of the ablated site opening size.

The need for access holes, which were used in previously fabricated probe substrates to facilitate complete lateral undercutting, has been eliminated by the addition of a heavily-doped buried layer beneath the epitaxial silicon. Figure 3 shows a comparison between structures undercut by sacrificial porous silicon with (Fig. 3a) and without (Fig. 3b) the use of a buried layer. Since the rate of pore formation increases with doping concentration, the use of a heavily-doped layer beneath the epi greatly increases lateral rate of pore formation. Without this buried layer, the formation of pores is quite isotropic and the entire thickness of the wafer may become porous in the etch time necessary to laterally undercut the probes. This makes the wafer quite fragile and subsequent processing very difficult.

Extensive characterization of the doping of the buried layer and the formation of the porous sacrificial layer has been conducted. The use of a p+ buried layer has been found to be preferable over an n+ layer for several reasons. Pores formed in p-type silicon are much smaller than those formed in n-type silicon and, as a result, p-type porous silicon leaves a much smoother surface when it is removed in room-temperature KOH (Fig. 4). Secondly, the use of an n+ buried layer in an n-type substrate results in electropolishing, or complete removal of the n+ layer, while the use of a p+ buried layer on a p-type substrate results in the formation of a porous layer. While electropolishing would be desirable for etching out devices in a single step, in the probe fabrication process, the sacrificial layer must be formed in the middle of the process and not removed until processing is complete. Figure

5 shows an n-type epi probe substrate that was partially undercut by forming porous silicon in a p+ layer beneath the probe. The p+ sacrificial porous layer was formed by etching the silicon wafer in 49% HF with a current density of approximately 40mA/cm^2 for 10 minutes. The sacrificial layer was then removed by etching in 10% KOH at room temperature for 5 minutes.

As a result of the above findings, the final process design utilizes a p+ buried layer in a p-type wafer substrate. The probes themselves are fabricated in p-type epitaxial silicon with an n-type outside layer. An n-well CMOS process is used to fabricate the circuitry. The porous sacrificial layer is formed just prior to the first metalization step and removed in KOH as the final step in the process. A mask set is currently being designed which will be used to fabricate active probes using this new micromachining process, and fabrication of these devices will begin early next quarter.

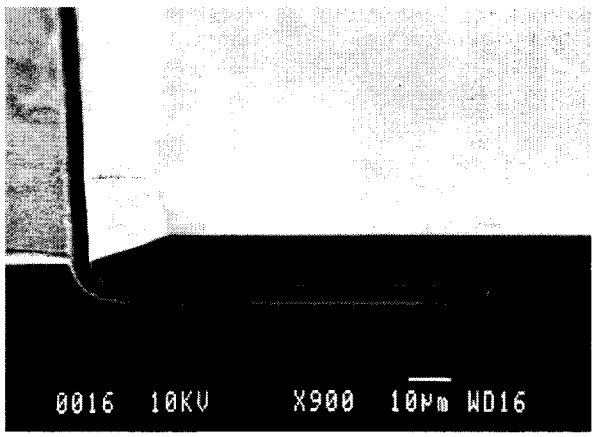

(a)

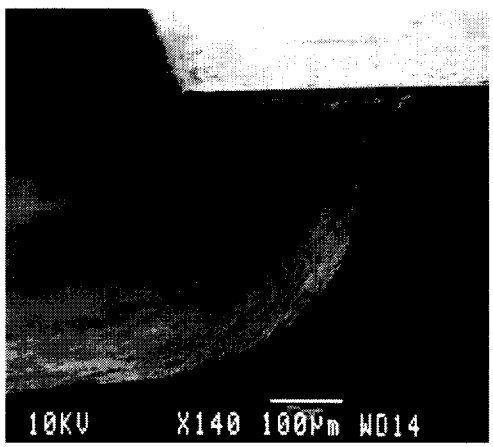

(b)

Fig. 3: Cross-sections of two structures partially undercut by anodic etching in HF, followed by sacrificial layer removal in KOH. The presence of a heavily-doped buried layer (a) greatly increases the lateral rate of pore formation with respect to the depth to which pores are formed. When no buried layer is used, pore formation is nearly isotropic (b).

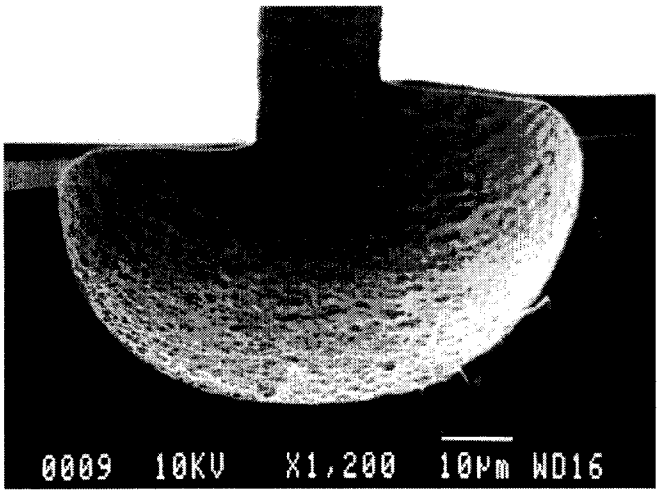

(a)

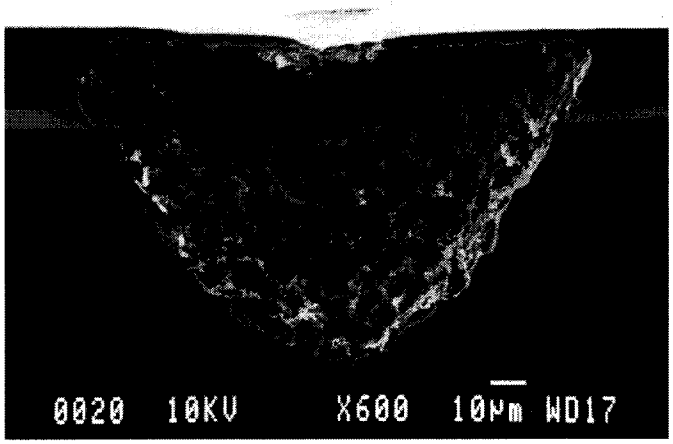

(b)

Fig. 4: Cross-sections of two wafers in which porous silicon was formed from access holes in a nitride mask, then removed in room-temperature KOH. P-type porous silicon (a), whose pores are on the order of nanometers apart, results in a much smoother surface when it is removed than does n-type porous silicon (b), whose pores are spaced as much as 1mm apart.

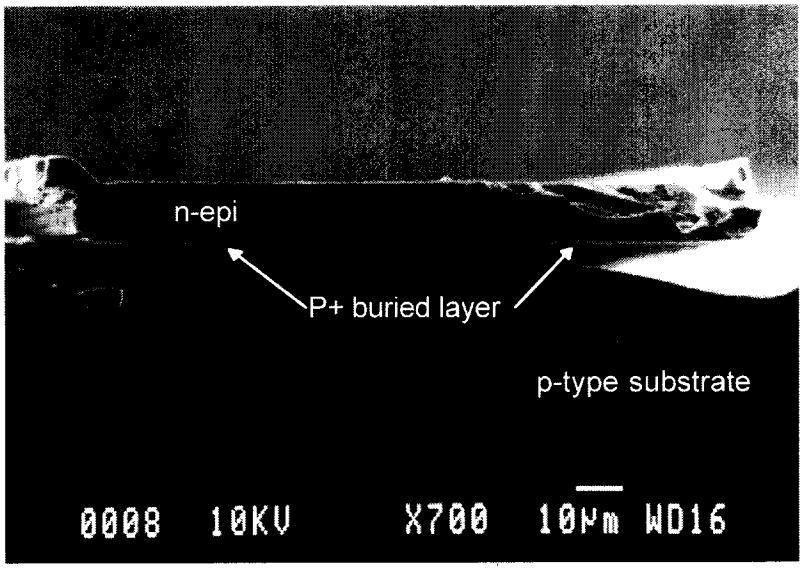

Fig. 5: Cross-section of a lightly-doped epitaxial silicon probe substrate partially undercut by a p-type porous silicon sacrificial layer. Porous silicon was formed in a p+ layer buried beneath the n-type epi in order to increase the rate of pore formation in the lateral direction. The porous sacrificial layer was then removed in room-temperature KOH.

4. Active Stimulating Probe Development

During the past quarter, work on the active stimulating probe has focused on refabricating two of the active stimulation probe mask sets, STIM-2B/3B and the STIM-2 mask set, which includes the STIM-1B, -2B, and -2 designs. These mask sets use up to 16 masking steps in the process, which includes the deep/shallow boron CMOS process and the 3-mask site process (STIM2B/3B). The CMOS circuitry was completed and tested on one wafer of the STIM2B/3B mask set. Testing has demonstrated that all of the circuitry on this probe is fully functional with performance close to design targets. The problem (high NMOS threshold voltage) that caused the failure of the last fabrication run has been completely eliminated, as expected from process simulation results performed to analyze the previous run.

STIM-2B

STIM-2B is a second-generation probe and is a version of our simplest active stimulating probe, STIM-1B. STIM-2B is a four-channel, 16-shank, 64-site probe which routes each of four externally-generated stimulus signals to 1 of the 16 sites in its respective site group. The fabrication of the CMOS circuitry has been completed and the digital functionality of the circuitry has been verified through testing. Testing of the on-chip analog recording amplifier has demonstrated that it too works quite well in spite of small variations in transistor device parameters. The variations in the process parameters across the wafer was actually quite low, and the yield appears to be very good. Every circuit tested appears to be functional. These findings are very encouraging.

The functionality of the STIM-2B probe is expected to provide an important tool for performing some key experiments by allowing acute and chronic stimulation access to relatively large volumes of neural tissue without the mechanical repositioning of the probe. This capability is realized by utilizing a 20b shift register to load four 4b site addresses which allow electronic positioning of four externally-generated stimulus currents. Each address is decoded by a 1-of-16 nand-type decoder to connect the addressed site to an analog input/output pad through a large CMOS passgate transistor. A newly added recording function is included and is addressed by a fifth bit included with the 4b site address. This fifth bit selects between stimulation mode and recording mode by selecting either a direct path to the I/O pad from the site or a path through an amplifier for recording from the same site. Each of the four I/O channels has its own dedicated amplifier so that the functionality of all of the channels are independent of each other except for the up-front data input circuitry. This probe was designed to be tolerant of process-induced variations in the device performance. The only portion of the probe that is device parameter sensitive is the amplifier used in the recording mode.

A photograph of the completed STIM-2B probe circuitry is shown in Fig. 6. Testing of the circuit blocks revealed that there were no significant problems with any of the device parameters. Both of the threshold voltages were found to be slightly higher than expected, but the small shifts do not appear to affect the performance significantly. The circuit test results will be discussed below. In spite of the thresholds being slightly high, the analog amplifiers worked quite well.

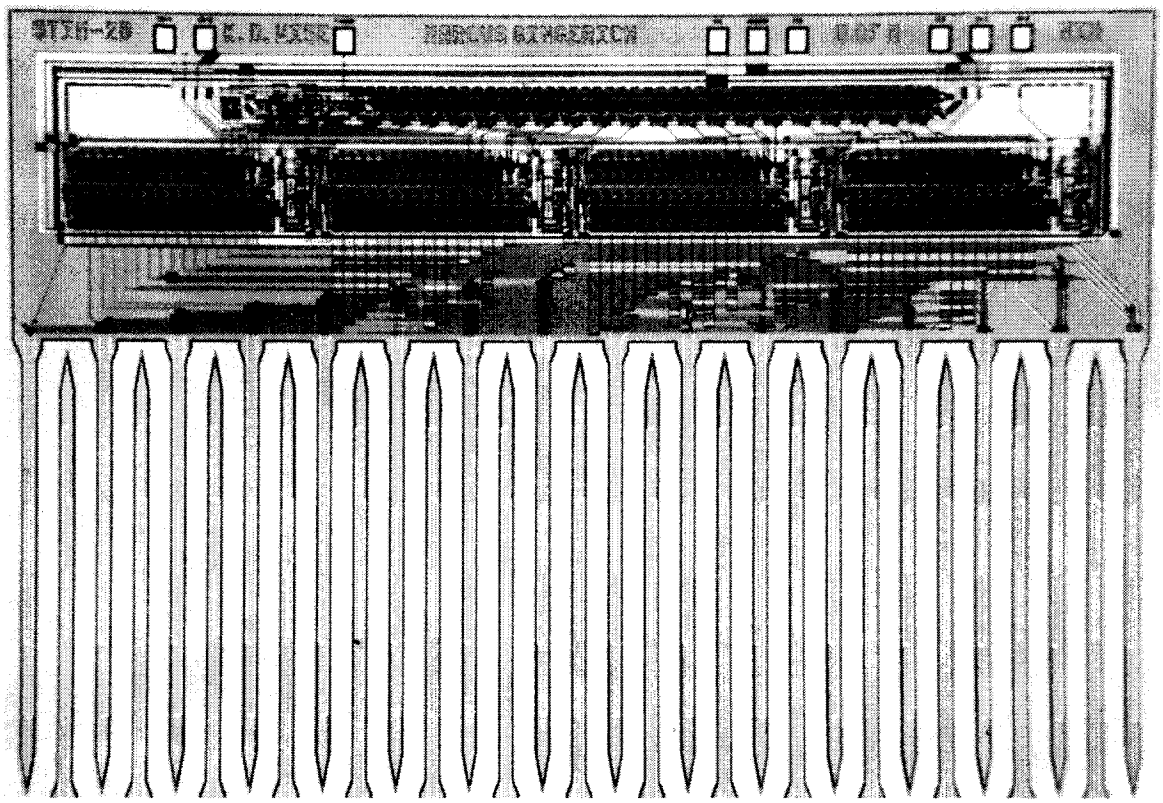

Fig. 6: A photograph of the STIM-2B probe. The shanks are on 400μm centers with four sites per shank.

STIM-3B

STIM-3B is a 3-dimensional probe that is an extension of the 2-D probe, STIM-2B, and is set up to allow use as a device in chronic experiments. There are no significant differences in the STIM-2B/3B probe designs but rather structural modifications to allow interconnection to a 3-D platform assembly and a few minor circuit enhancements to allow the addressing of multiple probes in a 3-D array.

The structural changes that are required, some of which can be seen in the photograph of the STIM-3B probe of Fig. 7, include the addition of 'wings' for 3-D stabilization and 'outriggers' with integrated beam-lead interconnects for assembly and lead transfer from each probe to the 3-D platform. Also seen in the photograph are the 45° slots on the wings which were designed such that a continuous trench would be etched from the front side of the probe even before the etch plane advances from the backside during the final release etch in EDP. As discussed in previous reports, the integrity of the circuit area was ensured by making the surrounding deep boron diffused rim wide enough so that the lateral undercut from the corners does not have time to reach the active circuit area. The newly developed corner protection technique of using dielectric bridges and the anisotropy of the EDP etchant was also used to help improve the yield. Previous tests have demonstrated the effectiveness of this technique.

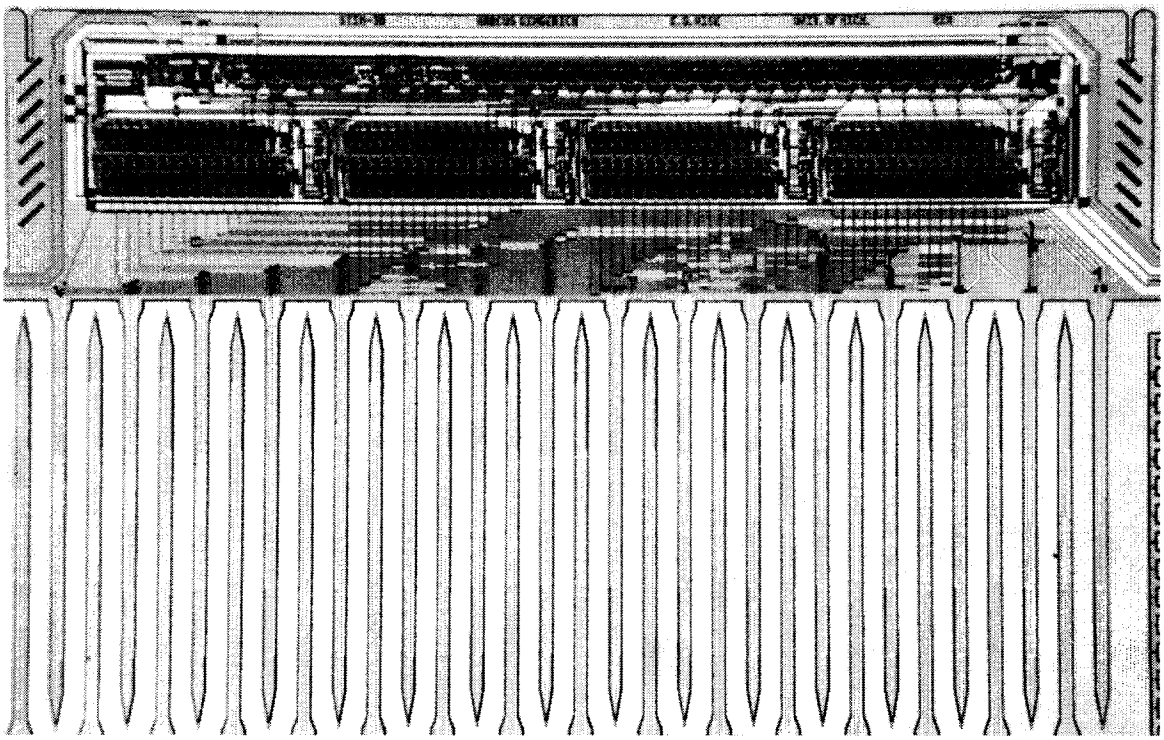

Fig. 7: A photograph of a STIM-3B probe. The probe contains mounting slots for the spacers associated with platform mounting. The outrigger "wings" containing the gold beam lead transfers are not shown in this photograph. The shanks are on 400μm centers with 4 sites per shank.

The minimal circuit changes necessary for realization of the STIM-3B probe included adding a 4b shift register which flags the selection of an I/O line via a large CMOS

passgate in the line. The last bit of the shift register is then buffered back out (Fig. 8 shows some of these circuits). This allows all the probes of a 3D system to share common analog I/O data lines, power lines, clock lines and y-addr (normal probe address) lines. The same y-addr is clocked into all the probes. Simultaneously, an x-addr (channel I/O enable) is clocked into the first probe and then daisy-chained to each successive probe in the array making an extended 'virtual register.' This allows for different size probe arrays with the only changes involving changes in the addresses provided by the external drive circuitry. This allows for a very flexible system with variable array size, inter-probe stimulation and almost any combination of four sites across the array. The only weakness is that the same I/O channel cannot be driven on more than one probe simultaneously with an independent stimulus current.

Circuit Test Results

As mentioned previously, the testing results on the new set of probes have been very good. The problems that have caused low yield in the past have been overcome. The contact resistances were all very low, with the highest being the contacts between the metal interconnect and the p+ source/drain regions, which averaged 3.50Ω/contact and a maximum of 4.13 Ω/contact. All of the other types of contacts were measured to be less than 1Ω/contact or at most slightly above. The PMOS and NMOS transistor threshold voltages were measured to be -1.08V and +1.12V, respectively, which are both slightly higher than the expected ±0.8V targets. These threshold voltages should not cause any significant changes in the overall functionality of the primarily digital circuitry of the STIM-2B/3B probes and also allow good functionality of the analog amplifiers.

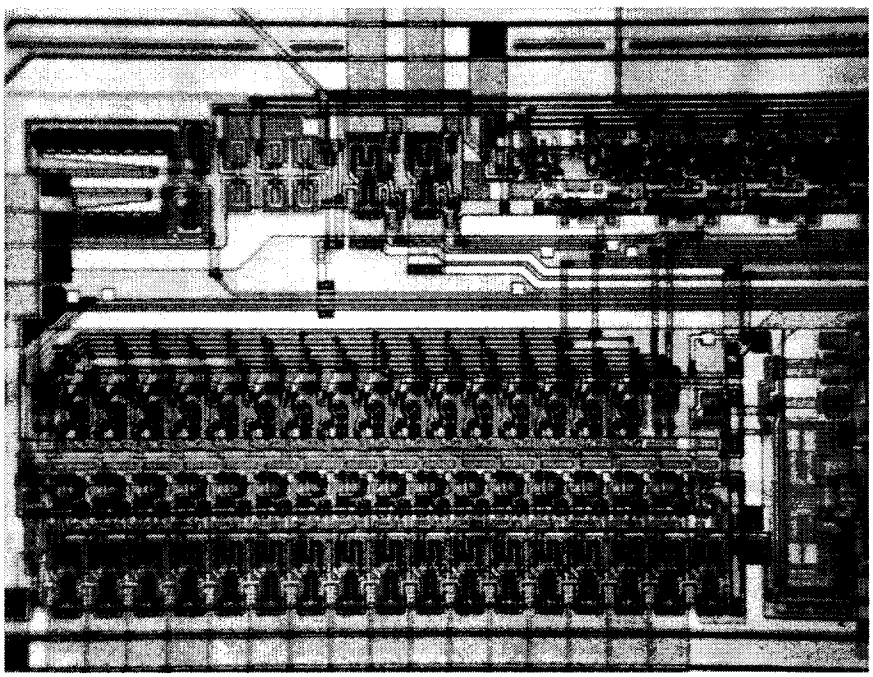

Fig. 8: A photograph of a section of the STIM-3B probe circuitry. The x-address output buffer can be seen at the upper left with input protection diode clamps next to it, some channel selection passgates and finally part of the 4b x-address shift register in the upper right. The lower section is filled by the 1-of-16 site selector and the amplifier in the lower right corner.

The functionality of the probe digital logic was demonstrated in the previous quarterly report, but a sample oscilloscope trace is shown below in Fig. 9. The top trace is the input clock signal, the middle trace is the input probe data, and the bottom trace is the signal which turns on the passgate for Site 2 of Channel A. In this case we see that it is turned on after two clock cycles as expected.

The functionality of the amplifier is demonstrated by the photograph shown in Fig. 10. The 1kHz 20mVp-p signal shown in the upper trace was input to the amplifier; an output of a little over 1Vp-p is observed in the lower trace. A complete characterization of the amplifier response is shown in Fig. 11, which shows the measured gain and phase response of the amplifier from 10Hz to 1MHz. The maximum gain measured is 42 dB.

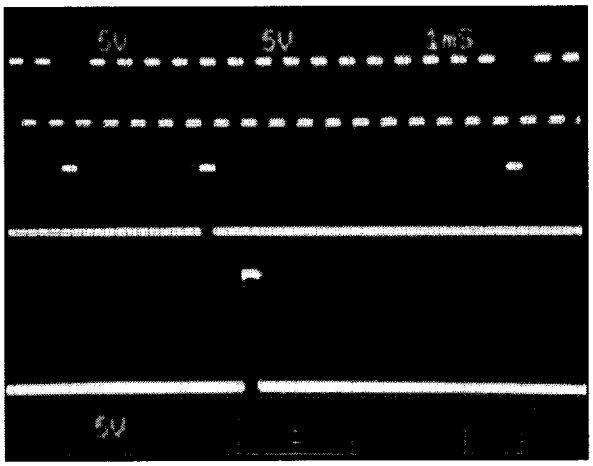

Fig. 9: A scope trace showing (top to bottom): the input clock; the input probe data; and the level-shifted output of bit-19 of the input shift register.

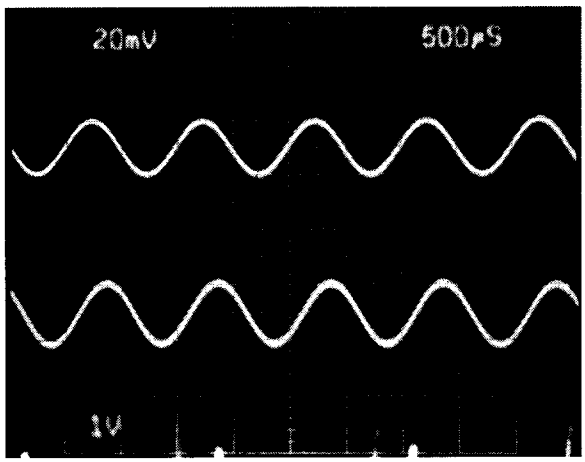

Fig. 10: A scope trace showing the 1kHz 20mVp-p signal at the input of one of the recording amplifiers (above) and the output signal (>1Vp-p) below.

Only one wafer has been metalized thus far, so only one wafer has been tested. Several of the wafers were dropped from the process just prior to the threshold implants so

that it will be fairly simple to make the necessary adjustments in the implant doses to zero in the threshold voltages on these wafers if we feel that it is necessary after the current wafer is completed. It is expected that the current wafer should be able to be run through the remainder of the process in another 2 weeks and then final testing will be performed to determine the status of the current process. No problems are anticipated since the next steps are all performed at low temperature and should have no effect on the CMOS circuitry. We feel we have the final etch-out process well in hand so that we should not see significant yield losses associated with that step. The combination of dielectric bridge corner protection and, if necessary, deep trench release acceleration, is expected to yield very good results from this final step.

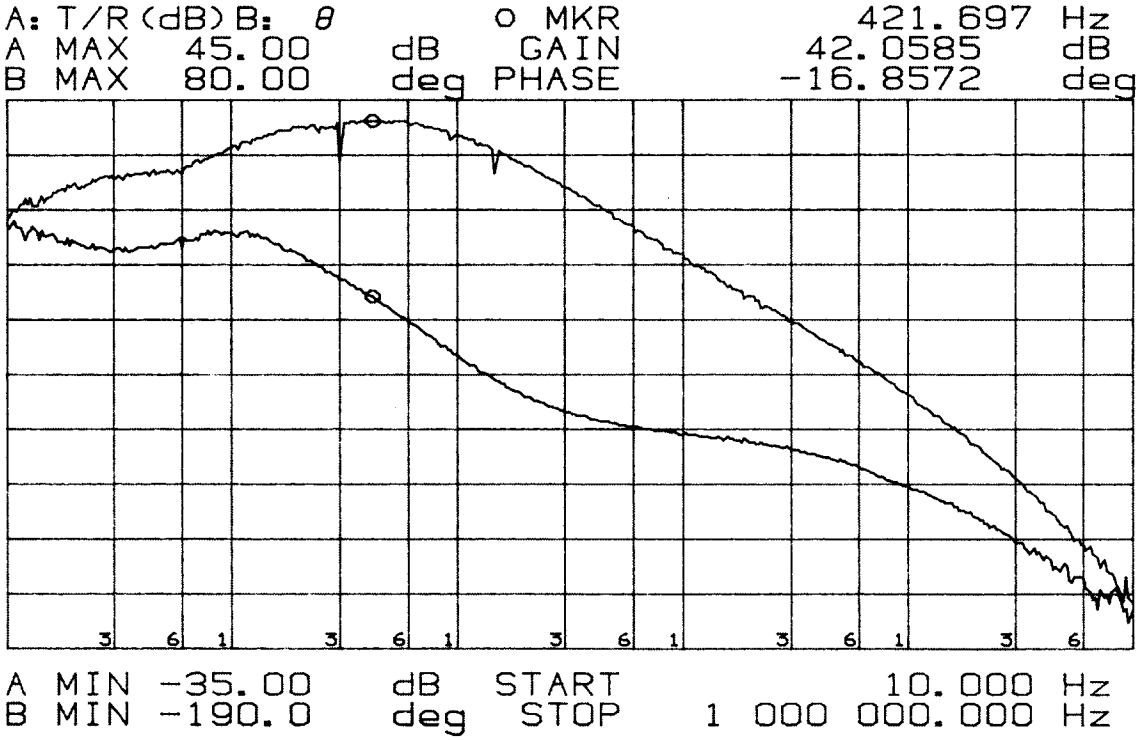

Fig. 11: The recording amplifier frequency response over the range from 10Hz to 1MHz with the gain (dB) on the top curve and the phase (deg.) on the bottom curve.

STIM-2 MASK SET

In addition to the STIM-2B/3B wafers that are nearing completion, three wafers from the STIM-2 mask set are also nearing completion as well as a some left prior to the threshold implant steps. They need to be metallized and then they can be tested as well. The good test results from the STIM-2B/3B wafer gives us reason to believe that these wafers should produce many working probes of the STIM-2, STIM-1B, and STIM-1A designs. These designs will be very useful in performing some significant experiments with multi-site stimulation electrodes. The different design features are explained in the following paragraphs.

STIM-1B is the simplest version of the active stimulating probes. The probe simply uses a four bit counter to select one of sixteen sites. The selected site is connected

to the analog data input pad through a pass-gate transistor. The counter is incremented by a positive pulse on the clock-in line. The counter can be reset to the first site by strobing the clock line negative. It is a monopolar version which simply acts as a current steering mechanism for an externally generated current. The functionality of this device is dependent mainly on the correct operation of the digital logic circuitry for selecting the correct site for current delivery. The lack of analog circuitry makes the design very robust in regard to the dependence on process parameters.

STIM-1A is a first-generation probe with the capability for on-chip bipolar current sourcing. The probe can source and sink current by selecting two of its sixteen $450\mu m^2$ sites, one as the current source and the other as the current sink, by clocking in a fifteen bit data word and latching it with a negative clock strobe. The first four bits specify the site address of the current sink electrode, the next four bits specify the site address of the current source electrode and the last seven bits specify the amplitude of the current to be driven, which can be as high as $254\mu A$ with a $2\mu A$ resolution.

STIM-2 is our second-generation probe in that it significantly extends the capabilities of the first generation probes in many areas. STIM-2 incorporates: 1) flexible interconnects, which allow the rear, circuit-containing, portion of the probe to be folded flat against the cortical surface to reduce the probe height above the cortical surface in an implant, 2) new circuitry for power and area reduction while increasing functionality, 3) a front end-selector which allows 8 of 64 sites to be driven simultaneously, thereby implementing electronic site positioning; and 4) compatibility with use in a multi-probe three-dimensional array.

Due to the problems associated with etching out these probes in the past, we will modify the field etch mask to incorporate dielectric bridge corner protection and perhaps a mask to accelerate probe release via a deep trench etch from the front of the wafer. The incorporation of these features should reduce the losses due to circuit undercutting during the final etch step to near zero.

In summary, the current run of STIM-2B/3B CMOS wafers was tested and found to function as expected. Some of the device parameters were precisely on target but were close enough so that even the analog amplifier works well. We still have the option of changing the thresholds on wafers that were held back just prior to the threshold implants to optimize the present process further. We anticipate completion of the post-CMOS processing and the final etch-out of these first probes within the next two weeks. These probes will then be used to perform some significant *in-vitro* and *in-vivo* tests during the coming quarter.

5. *External Stimulating Interface System Development*

In previous reports we have described the design and construction of an external interface system for active stimulating probes. A prototype of the hardware component of this system is now ready for use. We have also developed interface software for interacting with this hardware in the form of a textual, command-line interpreter. This software enables basic system testing and operation as well as simple stimulating tasks.

Our work during the past quarter has focused on the design and development of a graphical user interface as a front-end replacement for the existing software interface. The purpose behind this activity is to allow our software to be usable by both experienced users (via the command-line interface) as well as novice users who prefer a simpler and more

integrated approach. The low-level command line interpreter will still be available as a sub-function of the graphical user interface in order to enable any tasks that can not be performed with the current version of the software. Most of the development of this graphical interface is complete, and we expect to have functional software available early in the following quarter. The features of the graphical interface will be determined by the needs of users; hence, we expect that the development of this interface will be an ongoing process.

Our efforts during the remainder of the upcoming quarter will be split among several tasks. First, we expect to provide support for integrating our hardware with active stimulating probes and support for performing experiments with these probes. Second, we plan on refining our software to meet the emerging demands of these activities. Third, we intend to initiate the design and construction of a printed circuit board realization of our hardware. As our hardware currently only exists in prototype form on a wirewrap carrier, it has a limited lifetime as well as limitations on performance, such as maximum stimulation rate. For long term usage, we propose that a more robust implementation on a printed circuit board will enable faster and more reliable operation.

6. Conclusions

This program seeks to develop a family of two- and three-dimensional active stimulating probes for use in neural prostheses. Two active probes, STIM-1B (monopolar) and STIM-1A (bipolar) have been completed. A four-channel 64-site multipolar probe, STIM-2B is now being completed. This probe allows each of four externally-generated currents to be steered to one of 16 sites under the direction of a digital address delivered to the probe. A three-dimensional version of this probe, STIM-3B, is also nearing completion. Following these probes, the design of a 64-site 8-channel probe, STIM-2, will be iterated, and this probe will also be fabricated, completing this second-generation family of devices.

During the past quarter, we continued to explore the removal of parylene from iridium sites using laser ablation. Site areas ranging from $100\mu m^2$ to $400\mu m^2$ were created on a larger metal site using ablation. The surface was cleaned after ablation using an oxygen plasma, and the resulting sites were used for single-unit recording in cerebellum. The sites performed well, indicating that the ablation procedure is able to open sites in probes that have been coated with parylene. This allows the use of parylene as an outer conformal coating on penetrating probes as well as its use on ribbon-based electrode arrays suitable for cochlear prostheses. We have also completed process development on the possible use of a porous silicon layer for probe fabrication. This layer would be used under the basic probe structure and would permit release of the probe using a room-temperature front-side etch. The final process developed uses a p+ diffusion to produce the porous sacrificial layer. It allows circuitry to be distributed on the probe shanks as well as in the rear of the probe.

We have successfully fabricated a run of STIM-1A, -1B, -2, -2B, and -3B probes. As of this writing, one wafer of the -2B/3B probes has been taken to the completion of circuit processing and is found to be completely functional, including the per-channel recording amplifiers. We plan to release these probes from the wafer during the next two weeks and then to complete processing on the other probes. We then anticipate using the probes for a number of in-vivo tests before going back to iterate the design of STIM-2 to complete this second-generation family of probes.